

## 誌謝

首先，要感謝指導教授林宏洲老師這兩年的照顧指導，才成就了今日碩士學位的完成。除此之外，也要感謝中央化學所 賴重光老師、大同化工所 吳勛隆老師、交大電物所 趙如蘋萍老師審閱全文，並給予寶貴意見，使這篇論文更為完善。

當然，實驗室的大家更是幫助我許多，首推博仁學長，在我實驗遇到瓶頸時跳出來救了我一把；King 適時地給我鼓勵，阿之、瑜玲、家瑋也在後頭給我精神喊話，我才可以在碩二這年撐過去；也謝謝我碩士班的同窗好友煜證、老魏、阿沛妹，一起走過的兩年，當回頭想想也會覺得甜蜜；阿仁、三刀和龍哥謝謝你們無所抗拒的接受我任何要求，讓我實驗忙碌時多了你們這些小幫手輕鬆了許多；彥興、癡癡、曉萍、明修、Hari、Sahu、Patra、Sata 每一個人都在我身邊給我幫助，我都謹記在心。還有隔壁的張立休息室同胞，感謝你們平日的照顧，也讓實驗室有溫馨的感覺。

最後我要感謝我最親愛的家人們，謝謝你們給我衣食無缺的生活，讓我可以去追求我想要的生活-最疼我的爸爸、愛跟我吵架的媽媽，還有總是要酷的老哥，我真的很愛你們，謝謝你們一直包容任性的妹仔，此時此刻，我也該為自己負責任了。

謹以這份論文，獻給我最愛的人。

# 彎曲型氫鍵液晶材料摻雜金奈米粒子表面修飾彎曲型液晶分子之合成與應用

學生：張怡婷

指導教授：林宏洲 博士

國立交通大學材料科學與工程研究所碩士班

## 摘要

本實驗成功合成出硬核中心為單苯環、雙苯環結構的彎曲型氫鍵液晶，除了規劃一系列香蕉型氫鍵液晶系統，以得到一個較寬廣的 SmCP<sub>F</sub> phase 溫寬系統 (SiA-PyBVF<sub>14</sub>)，再將所得到的彎曲型氫鍵液晶材料摻雜金奈米粒子，而奈米金粒子的表面是受到彎曲型液晶藉由硫醇鍵修飾，透過 POM、DSC、XRD 及光電量測來探討摻雜金奈米粒子前後的液晶行為。並成功利用電場誘導香蕉型氫鍵液晶具有單方向的規則排列，並由 In-Situ 之通電的 XRD 觀察其排列。

# **Synthesis and Applications of Hydrogen-Bonded Bent Core Liquid Crystal Hosts Doped with Gold Nanoparticles Decorated with Bent Core Liquid Crystal Surfactants.**

Student: Yi-Ting Chang

Advisor: Dr. Hong-Cheu Lin

Department of Materials Science and Engineering  
National Chiao Tung University

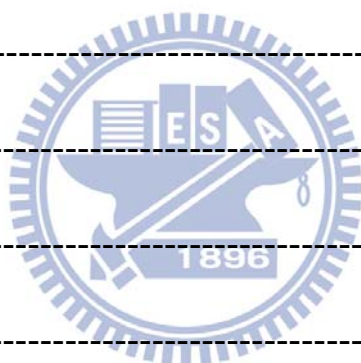
## Abstract

In this research, we successfully synthesized a series of banana-shaped hydrogen-bonded liquid crystalline molecules, containing either single or double-membered benzene rings, in order to obtain broader temperature ranges of  $\text{SmCP}_F$  phase (**SiA-PyBVF<sub>14</sub>**). Furthermore, these banana-shaped hydrogen-bonded liquid crystalline molecules were doped with gold nanoparticles, which were surface-modified by banana-shaped liquid crystalline surfactant through thiol bonding. Correspondingly, we investigated the liquid crystalline behavior both before and after doping of nanoparticles by dint of a variety of instruments, such as POM, DSC, XRD and optical-electro measurement. More importantly, we acquired a well-structured liquid crystalline phase by an in-situ electric-field induction monitored through XRD.

誌謝-----	I
摘要-----	II
英文摘要-----	III
目錄-----	IV
圖目錄-----	VI
表目錄-----	XII
第一章序論-----	1
1-1 前言-----	2
1-2 液晶簡介	
1-2-1 液晶的發現-----	2
1-2-2 液晶的分類-----	3
1-2-3 液晶相的鑑定方法-----	12
1-3 香蕉型液晶	
1-3-1 香蕉型液晶簡介-----	14
1-3-2 香蕉型液晶分子設計-----	18
1-3-3 鐵電與反鐵電行為-----	18
1-3-4 對掌性特徵與鑑定方式-----	21
1-3-5 自發極化值的測量-----	25
1-4 超分子(Supramolecular)氫鍵型液晶-----	26



1-5 含矽之寡分子香蕉型液晶-----	27
1-6 奈米材料	
1-6-1 奈米金屬材料簡介-----	33
1-6-2 奈米金粒子的製備方法-----	33
1-6-3 奈米金粒子表面電漿共振( Surface Plasmon Resonance)原理 -----	36
1-6-4 含奈米金粒子之彎曲型液晶分子-----	40
1-7 文獻回顧與研究動機-----	42
第二章實驗部分-----	45
2-1 實驗藥品-----	46
2-2 實驗儀器-----	48
2-3 合成流程-----	53
2-4 合成步驟-----	57
2-5 奈米金粒子的製備-----	91
2-6 摻雜流程-----	91
2-7 液晶元件製作流程-----	92
2-8 光電量測-----	93
第三章結果與討論-----	94
3-1 硬核中心為單苯環、雙苯環結構的彎曲型氫鍵液晶-----	95



3-1-1	紅外線光譜分析-----	95
3-1-2	POM 觀察-----	97
3-1-3	DSC 量測-----	100
3-1-4	Powder XRD 量測-----	103
3-2	香蕉型氫鍵液晶與奈米金粒子摻雜研究-----	107
3-2-1	穿透式電子顯微鏡分析-----	107
3-2-2	POM 觀察-----	108
3-2-3	DSC 量測-----	111
3-2-4	Powder XRD 量測-----	113
3-2-5	光電量測-----	115
3-2-6	以彎曲核液晶分子修飾的奈米金粒子作為玻璃表面配向研究-----	119
3-3	結論-----	121
3-4	未來展望-----	122
	參考文獻-----	123
附錄 A	系列四彎曲型氫鍵液晶的 DSC 掃描圖-----	129
附錄 B	吡啶基與羧酸基分子 $^1\text{H-NMR}$ 圖譜-----	131
附錄 C	吡啶基與羧酸基分子 EA、MS 圖譜-----	134
	圖目錄	

Fig. 1-2-1.1 安息香酸膽固醇酯-----	3
Fig. 1-2-2.1 液向型液晶-----	5
Fig. 1-2-2.2 單變型液晶-----	5
Fig. 1-2-2.3 雙變型液晶-----	6
Fig. 1-2-2.4 重現型液晶-----	6
Fig. 1-2-2.5 向列相分子排列圖-----	7
Fig. 1-2-2.6 droplet 紋理圖與 schilieren 狀紋理圖-----	8
Fig. 1-2-2.7 層列相分子排列圖-----	8
Fig. 1-2-2.8 SmA 相分子排列圖-----	9
Fig. 1-2-2.9 SmA 相紋理圖-----	9
Fig. 1-2-2.10 SmC 相分子排列圖-----	10
Fig. 1-2-2.11 SmA 相轉變成 SmC 相的紋理圖-----	10
Fig. 1-2-2.12 分子長軸傾斜示意圖-----	11
Fig. 1-2-4.1 偏光顯微鏡設計圖及其原理-----	13
Fig. 1-2-4.2 分子在層內傾斜之角度示意圖-----	14
Fig. 1-3-1.1 盤狀堆疊、層狀堆疊與三維結構螺旋堆疊形式-----	15
Fig. 1-3-1.2 彎曲型液晶分子基本結構-----	15
Fig. 1-3-3.3 香蕉型液晶分子之構型與其示意圖-----	17
Fig. 1-3-1.4 香蕉型分子堆疊基本行為-----	17

Fig. 1-3-1.5 對掌性質的誘發點：分子傾斜方向與偶極方向-----	17
Fig. 1-3-2.1 彎曲分子的基本架構-----	18
Fig. 1-3-3.1 鐵電與反鐵電行為的示意圖-----	19
Fig. 1-3-3.2 方波、正交偏光板、在POM下觀察到的十字刻痕，(a) 負電場下鐵電狀態 ( $\text{SmC}_S\text{P}_F$ ); (b) 去除電場反鐵電狀態 ( $\text{SmC}_A\text{P}_A$ ) and (c) 正電場下鐵電狀態 ( $\text{SmC}_S\text{P}_F$ ) 圖解分子在圓的區域擁有距的層列層，就如同圖中的排列-----	20
Fig. 1-3-3.3 鐵電與反鐵電在一般三角波與修飾三角波下的回應電流表現-----	21
Fig. 1-3-4.1 $\text{SmC}_A\text{P}_A$ 基本態轉 $\text{SmC}_S\text{P}_F$ 激發態-----	23
Fig. 1-3-4.2 $\text{SmC}_S\text{P}_F$ 基本態轉反向 $\text{SmC}_S\text{P}_F$ 激發態-----	23
Fig. 1-3-4.3 $\text{SmC}_A\text{P}_F$ 基本態轉反向 $\text{SmC}_A\text{P}_F$ 激發態-----	23
Fig. 1-3-4.4 $\text{SmC}_S\text{P}_A$ 基本態轉反向 $\text{SmC}_A\text{P}_F$ 激發態-----	24
Fig. 1-3-4.5 藉由旋轉偏光板而得知有不同對掌區域的紋理圖-----	24
Fig. 1-3-5.1 FLC 與 AFLC 在三角波法下所測得的不同圖形-----	25
Fig. 1-3-5.2 化合物1df 的三角波電流回應峰圖-----	26
Fig. 1-4.1 超級複合分子液晶基之結構圖-----	27
Fig. 1-5.1 含矽(氧)元素之彎曲型液晶分子-----	28



Fig. 1-5.2(a)單邊引入矽氧基團之對稱彎曲型分子；(b)雙邊引入矽氧基團之不對稱彎曲型分子-----	29
Fig. 1-5.3 (a)中間引入矽氧基之彎曲型雙分子結構；(b)彎曲型分子引入於含矽氧基之特殊分子結構中的設計-----	31
Fig. 1-5.4 彎曲型分子側邊硬段取代基的影響-----	32
Fig. 1-6-2.1 以硫醇基丙酸鹽 (mercaptopropionate) 為穩定劑製備奈米金之步驟-----	34
Fig. 1-6-2.2 硫醇包覆奈米金之取代反應示意圖-----	35
Fig. 1-6-3.1 表面電漿波示意圖-----	37
Fig. 1-6-3.2 金奈米粒子之粒徑與表面之電漿吸收峰的關係圖-----	40
Fig. 1-6-4.1 含奈米粒子彎曲型液晶分子-----	41
Fig. 1-7.1 具有不對稱氫鍵位置的 SmCP phase 溫寬探討-----	44
Fig. 2-5.1 合成奈米金粒子流程圖-----	91
Fig. 2-6.1 將液晶材料灌進試片流程：(a). 加熱至 isotropic (b). 抽真空 (c) 破真空回室溫-----	92
Fig. 2-7.1 測量電流回應值的實驗裝置-----	93
Figure 3-1-1.1 FTIR spectra of (a) pyridyl tail of bent core liquid crystal (PyBVF <sub>14</sub> ), (b) hydrogen-bonded complex SiA-PyBVF <sub>14</sub> , (c) small	

benzoic acid, SiA. -----96

Fig. 3-1-2.1 POM textures at the cooling process: (a) the polar smectic phase of complex **SiA-PyBVF14** at 127 °C; (b) at 100 °C-----97

Fig. 3-1-2.2 POM textures of SiA-PyBVF<sub>14</sub> by applying electric fields (V<sub>pp</sub> = 300 V) -----98

Fig. 3-1-2.3 Sequential structural transformations of compound SiA-PyBVF<sub>14</sub> from [SmC<sub>s</sub>P<sub>F</sub>]<sub>a</sub>P<sub>S</sub> to SmC<sub>s</sub>P<sub>F</sub> observed by switching current responses and texture changes with temperature and time in a 7.5 μm ITO-coated cell (300 V, 100 Hz): (a, b) only [SmC<sub>s</sub>P<sub>F</sub>]<sub>a</sub>P<sub>S</sub> at 117.8 °C ;(c, d) transformation from [SmC<sub>s</sub>P<sub>F</sub>]<sub>a</sub>P<sub>S</sub> to SmC<sub>s</sub>P<sub>F</sub> at 91.9 °C; (e, f) at 88.9 °C; (i, j) transformation from [SmC<sub>s</sub>P<sub>F</sub>]<sub>a</sub>P<sub>S</sub> to SmC<sub>s</sub>P<sub>F</sub> at 83.0 °C; (k, l) incomplete transformation from [SmC<sub>s</sub>P<sub>F</sub>]<sub>a</sub>P<sub>S</sub> to SmC<sub>s</sub>P<sub>F</sub> at 78.0 °C. The brightness in pictures is not scaled, because of different exposure times.

-----100

Fig. 3-1-2.4 Proposed modes of organization of compound SiA-PyBVF<sub>14</sub> depending on the conditions., (a) Apparently anticlinic and synpolar [SmC<sub>s</sub>P<sub>F</sub>]<sub>a</sub>P<sub>S</sub> structure as obtained by cooling under an applied AC-voltage, (b) Uniform synclinic and synpolar SmC<sub>s</sub>P<sub>F</sub> structure as obtained upon cooling under an applied AC-voltage with sufficient time.

-----100

Fig. 3-1-3.1 Phase diagram upon 2<sup>nd</sup> cooling of **PyBIVSi-FA**<sub>12</sub>, **SiA-PyBVF**<sub>14</sub> and **A**<sub>12</sub>-**SiA-PyBVF**<sub>14</sub>-----103

Fig.3-1-4.1 XRD patterns of (a) **SiA-PyBVF**<sub>14</sub> at 130 °C,cooling, (b) **A**<sub>12</sub>-**PyBVF**<sub>14</sub> at 100 °C,cooling-----105

Fig.3-1-4.2 以電場誘導 SiA-PyBVF<sub>14</sub> 分子排列示意圖-----106

Fig.3-1-4.3 Powder X-ray 2D pattern of complex **SiA-PyBVF<sub>14</sub>** in small and wide angle by applying electric field. -----107

Fig.3-2-1.1 TEM images of gold nanoparticles with (a) scale bar is 20 nm and (b) 10 nm. -----108

Fig. 3-2-2.1 POM textures at the cooling process: (a) the polar smectic phase of complex **Au-SiA-PyBVF<sub>14</sub>** at 129 °C; (b) at 97 °C-----109

Fig.3-2-2.2 Sequential structural transformations of compound SiA-PyBVF<sub>14</sub> from [SmC<sub>s</sub>P<sub>F</sub>]<sub>a</sub>P<sub>S</sub> to SmC<sub>s</sub>P<sub>F</sub> observed by switching current responses and texture changes with temperature and time in a 7.5 μm ITO-coated cell (300 V, 100 Hz): (a, b) only [SmC<sub>s</sub>P<sub>F</sub>]<sub>a</sub>P<sub>S</sub> at 113.7 °C ;(c, d) transformation from [SmC<sub>s</sub>P<sub>F</sub>]<sub>a</sub>P<sub>S</sub> to SmC<sub>s</sub>P<sub>F</sub> at 104.8 °C; (e, f) at 102.5 °C; (i, j) transformation from [SmC<sub>s</sub>P<sub>F</sub>]<sub>a</sub>P<sub>S</sub> to SmC<sub>s</sub>P<sub>F</sub> at 95.3 °C; (k, l) incomplete transformation from [SmC<sub>s</sub>P<sub>F</sub>]<sub>a</sub>P<sub>S</sub> to SmC<sub>s</sub>P<sub>F</sub> at 83.3 °C. The brightness in pictures is not scaled, because of different exposure times. -----111

Fig. 3-2-3.1 Phase diagram upon 2<sup>nd</sup> cooling of **SiA-PyBVF<sub>14</sub>** and **Au-SiA-PyBVF<sub>14</sub>**-----112

Fig.3-2-4.1 XRD patterns of **Au-SiA-PyBVF<sub>14</sub>** at 100 °C,cooling-----113

Fig.3-2-4.2 Powder X-ray 2D pattern of complex Au-SiA-PyBVF<sub>14</sub> in small and wide angle by applying electric field. -----115

Fig.3-3-5.1 P<sub>s</sub> values as a function of applied voltages (a) SiA-PyBVF<sub>14</sub> as T = 95°C、f = 100 Hz; (b) Au-SiA-PyBVF<sub>14</sub> as T = 108°C、f = 100 Hz.-----116

Fig.3-2-5.2 Switching current responses of SiA-PyBVF<sub>14</sub> by applying a triangular wave (in antiparallel rubbing cells with 7.5 μm thickness. (V<sub>pp</sub> = 300 V、f = 100 Hz、R = 3 KΩ、T = 89 °C) -----116

Fig.3-2-5.2 Switching current responses of complex SiA-PyBVF<sub>14</sub> under the modified triangular wave method at V<sub>pp</sub> = 300 V、f = 100 Hz、R = 3 KΩ, (a)T = 89 °C (SmCP phase); (b) T = 65 °C (crystal solid state)-----118

Fig.3-2-5.3 Switching current responses of Au-SiA-PyBVF<sub>14</sub> by applying a triangular wave (in antiparallel rubbing cells with 7.5 μm thickness.(V<sub>pp</sub> = 300 V、f = 100 Hz、R = 3 KΩ、T = 105 °C) -----118

Fig.3-2-6.1 (a) surface alignment by gold nanoparticles decorated with bent core liquid crystal surfactants; (b) powder x-ray 2D pattern at small and wide angle. -----119

Fig.3-2-6.1 (a) (b) (c) ESCA analysis for bent core LC on glass-----120

表目錄

Table 1-2-2.1 液晶的分類-----4

Table 1-2-2.2 液晶形成方式分類圖-----4

Table 3-1-3.1 Phase transition temperatures and enthalpies of hydrogen-bonded complex-----102

Table 3-1-4.1 XRD data of hydrogen-bonded bent core liquid crystal--105

Table 3-2-3.1 Phase transition temperatures and enthalpies of SiA-PyBVF<sub>14</sub> and Au-SiA-PyBVF<sub>14</sub>-----112

Table 3-2-4.1 XRD data of SiA-PyBVF<sub>14</sub> and Au-SiA-PyBVF<sub>14</sub>-----114